

1 How to cite this published article:

2
3 Nechyporchuk, O.; Kolman, K.; Bridarolli, A.; Odlyha, M.; Bozec, L.; Oriola, M.;
4 Campo-Francés, G.; Persson, M.; Holmberg, K.; Bordes, R. On the Potential of Using
5 Nanocellulose for Consolidation of Painting Canvases. *Carbohydrate Polymers* **2018**,
6 *194*, 161–169. doi: 10.1016/j.carbpol.2018.04.020.

7
8 **On the potential of using nanocellulose for consolidation of painting canvases**

9 Oleksandr Nechyporchuk ^{a,1,*}, Krzysztof Kolman ^{a,2}, Alexandra Bridarolli ^b, Marianne Odlyha ^b,
10 Laurent Bozec ^b, Marta Oriola ^c, Gema Campo-Francés ^c, Michael Persson ^{a,d}, Krister Holmberg ^a,
11 Romain Bordes ^{a,*}

12 ^a Department of Chemistry and Chemical Engineering, Applied Surface Chemistry, Chalmers
13 University of Technology, 412 96 Gothenburg, Sweden

14 ^b Department of Biological Sciences, Birkbeck College, University of London, Malet Street,
15 Bloomsbury, London WC1E 7HX, United Kingdom

16 ^c Department of Arts and Conservation, Faculty of Fine Arts, University of Barcelona, C/Pau
17 Gargallo, 4, 08028 Barcelona, Spain

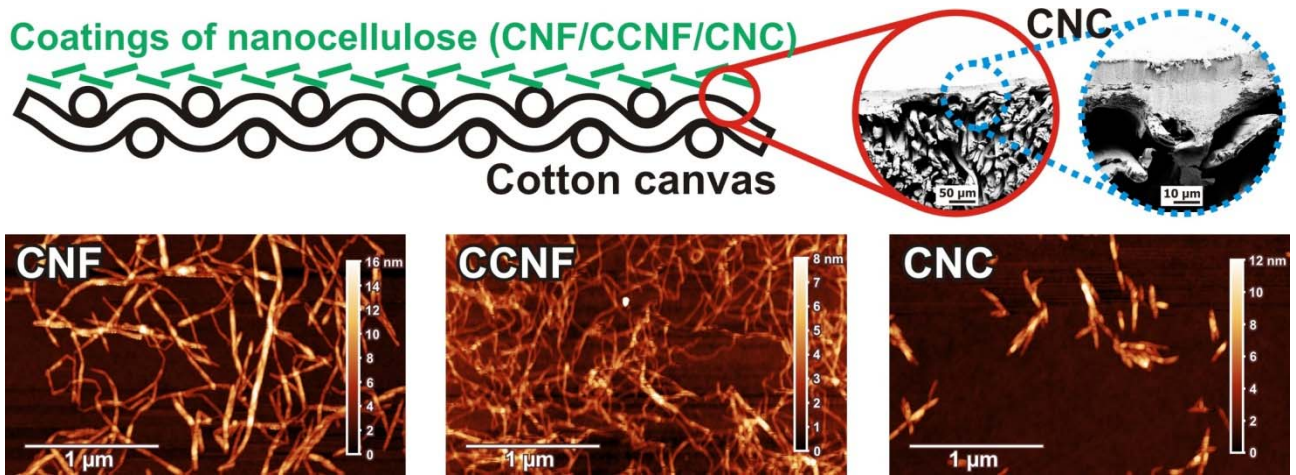
18 ^d AkzoNobel Pulp and Performance Chemicals AB, Sweden

19 ¹ Present address: Swerea IVF AB, Box 104, SE-431 22 Mölndal, Sweden

20 ² Present address: Department of Chemistry and Molecular Biology, University of Gothenburg,
21 Göteborg, Sweden

22 * Corresponding authors: oleksandr.nechyporchuk@swerea.se (O.N.); bordes@chalmers.se (R.B.)

23



25

26 **Abstract**

27 Nanocellulose has been recently proposed as a novel consolidant for historical papers. Its use for
 28 painting canvas consolidation, however, remains unexplored. Here, we show for the first time how
 29 different nanocelluloses, namely mechanically isolated cellulose nanofibrils (CNF),
 30 carboxymethylated cellulose nanofibrils (CCNF) and cellulose nanocrystals (CNC), act as a bio-
 31 based alternative to synthetic resins and other conventional canvas consolidants. Importantly, we
 32 demonstrate that compared to some traditional consolidants, all tested nanocelluloses provided
 33 reinforcement in the adequate elongation regime. CCNF showed the best consolidation per added
 34 weight; however, it had to be handled at very low solids content compared to other nanocelluloses,
 35 exposing canvases to larger water volumes. CNC reinforced the least per added weight but could be
 36 used in more concentrated suspensions, giving the strongest consolidation after an equivalent
 37 number of coatings. CNF performed between CNC and CCNF. All nanocelluloses showed better
 38 consolidation than lining with synthetic adhesive (Beva 371) and linen canvas in the elongation
 39 region of interest.

40

41 **Keywords**

42 Conservation, restoration, consolidation, easel paintings, cellulose nanofibrils (CNF), cellulose
 43 nanocrystals (CNC)

44

45 **1 Introduction**

46 Painting canvases made from natural fibers (*e.g.*, linen, hemp, cotton or jute), used by artists as
 47 painting support, age over time. The ageing occurs due to temperature and humidity variations, and
 48 hence the dimensional changes of the painting mounted on a stretcher (Hedley, 1988; Hendrickx,
 49 Desmarais, Weder, Ferreira, & Derome, 2016), as well as chemical processes caused by acidity,
 50 which originate from primers, paints, glues and absorption of acidic gases from the environment

51 (Ryder, 1986; Oriola et al., 2014). The ageing results in canvas degradation, particularly the
52 reduction of its mechanical properties, which may lead to cracking of the paint layer as well as
53 accidental tears of the canvas, resulting in irreversible damage of the painting.

54 In order to consolidate degraded canvases two options can be used: (i) consolidating the original
55 canvas with an adhesive and (ii) lining of the original canvas with a new one, i.e. gluing the new
56 canvas over the old one (Stoner & Rushfield, 2012). In both strategies, the damaged substrate on the
57 back side of the painting is treated by an adhesive, which may be natural, such as animal glue and
58 glue-paste, or synthetic, such as acrylic (Plexisol PB550, Paraloid B72 or Plextol B500) or complex
59 wax-resin formulations (Beva 371) (Berger, 1972; Ackroyd, 2002; Ploeger et al., 2014). Generally,
60 water-based adhesives are less favorable due to the hygroscopic character of the cellulosic canvas.
61 Swelling and shrinkage of the canvas occur as a response to interactions with water, resulting in
62 dimensional changes of the painting. The choice of proper material for canvas restoration is a major
63 concern for conservators and the ideal properties of such materials are still under debate. One of the
64 opinions with respect to lining and lining adhesive is to provide the painting with a stiffer support to
65 which the mechanical stress is transferred (Ackroyd, 2002; Young, 1999; Berger & Russell, 1988).
66 This reduces the load accumulated in the paint layer and minimizes the future degradation of the
67 painting. At the same time, it is important to allow elongation of the lining from 0.3 to 3.0%, which
68 is the elongation range to which paintings are exposed when mounted on a stretcher. It varies
69 depending on the type of canvas, warp or weft direction, the pigments used and the age of the
70 painting (Mecklenburg, 1982, 2005; Mecklenburg & Fuster Lopez, 2008).

71 Lining has traditionally been used for canvas restoration. However, with the growing interest in
72 methods that provide minimal intervention of the painting, other treatments have become popular in
73 the last decades (Ackroyd, Phenix, & Villers, 2002; Villers, 2004). The alternative treatments
74 become favorable mainly due to the issues of reversibility, aesthetic concerns, excess of added new
75 materials and no access to the original canvas with a lining. Another reason is that some of the
76 widely used synthetic adhesives, such as Beva 371, are questionable from health and environmental
77 point of view due to their toxicity (Bianco et al., 2015). Some synthetic adhesives, such as
78 poly(vinyl acetate), promote canvas degradation due to acidic products formed during their own
79 degradation (Chelazzi et al., 2014) and are therefore no longer used. These concerns have resulted
80 in an increased use of natural polymers, such as animal or fish glue, for canvas reinforcement
81 (Ackroyd, 2002).

82 The degraded canvas generally possesses defects at different length scales, *e.g.*, fiber cracks on
83 the micrometer scale and depolymerization of cellulose chains on the nanometer scale. In order to
84 restore the mechanical properties of the original canvas, these issues should be tackled (Kolman,
85 Nechyporchuk, Persson, Holmberg, & Bordes, 2017). In addition to the physico-chemical

86 properties of the canvas fibers, the morphology of woven fabric has a strong influence on the
87 mechanical properties (Young & Jardine, 2012). Taking into consideration that the paint layer, as
88 well as the ground or size, are much stiffer than the canvas, the conservation treatment may aim at
89 an efficient reinforcement for the canvas, rather than at restoration of the original properties,
90 including high stretchability and flexibility, as these properties have been lost with the application
91 of the different preparative layers. In parallel to the mechanical reinforcement, deacidification of the
92 canvas needs to be carried out in order to arrest further degradation (Giorgi, Dei, Ceccato,
93 Schettino, & Baglioni, 2002).

94 In the recent development of cellulose-based materials, nanocellulose has emerged and generated
95 a strong interest, often due to its unique mechanical properties. Nanocellulose can be divided into
96 three main categories: (i) cellulose nanocrystals (CNC), also referred to as nanocrystalline cellulose
97 (NCC) or cellulose whiskers (Habibi, Lucia, & Rojas, 2010; Rånby, 1949); (ii) cellulose nanofibrils
98 (CNF), also known as nanofibrillated cellulose (NFC) or microfibrillated cellulose (MFC) (Turbak,
99 Snyder, & Sandberg, 1983; Nechyporchuk, Belgacem, & Bras, 2016), and (iii) bacterial
100 nanocellulose. CNC and CNF are much more common, since they are produced by delamination of
101 cellulose microscopic fibers (generally, from wood) into nanomaterial (top–down process), whereas
102 bacterial nanocellulose is generated by a buildup (bottom–up process) from low molecular weight
103 sugars by bacteria (Nechyporchuk, Belgacem, & Bras, 2016). Bacterial cellulose is produced in the
104 form of biofilms (pellicles) of determined dimensions that contain interconnected nanofibrils
105 (Klemm, Heublein, Fink, & Bohn, 2005), whereas CNC and CNF are separate nanoparticles, thus
106 their deposition is not limited by the physical dimensions of the artifacts. In order to deposit
107 bacterial nanocellulose from suspensions, post-fibrillation should be performed.

108 The different types of nanocellulose present appealing features for the purpose of canvas
109 consolidation: they have high strength and form transparent/translucent and lightweight films. Their
110 non-toxic character and non-abrasiveness for processing equipment, as well as renewable and
111 biodegradable character, are additional features of interest for the field. Nanocellulose also has a
112 large surface area and there are well-developed methods for its surface modification (Habibi et al.,
113 2010; Moon, Martini, Nairn, Simonsen, & Youngblood, 2011; Nechyporchuk, Belgacem, & Bras,
114 2016). Reinforcing a cellulosic canvas with a material of similar nature can be beneficial for future
115 preservation of canvas paintings.

116 The interest in using nanocellulose for restoration of cellulosic materials has been increasing
117 lately. Nanocellulose has recently been employed for consolidation of historical papers (Santos et
118 al., 2015; Dreyfuss-Deseigne, 2017; Völkel, Ahn, Hähner, Gindl-Altmutter, & Potthast, 2017).
119 Bacterial nanocellulose has been also reported for reinforcement of historical silk fabrics (Wu, Li,

120 Fang, & Tong, 2012). To the best of our knowledge, the use of nanocellulose for consolidation of
121 painting canvases remains unexplored.

122 In this work, different types of nanocellulose, namely mechanically isolated cellulose nanofibrils
123 (CNF), carboxymethylated cellulose nanofibrils (CCNF) and cellulose nanocrystals (CNC), were
124 tested and compared in terms of structural reinforcement of degraded canvases. The mechanical
125 properties of newly prepared and real paintings were first studied to determine the elongation
126 regime where canvas consolidation should act. Then, model aged canvases were treated with
127 different nanocellulose-based formulations to investigate their film-forming properties on canvases
128 and their response to static and periodic uniaxial stress at different relative humidity values. The
129 reinforcing effect of the nanocelluloses was also compared with that obtained with different
130 traditional consolidants.

131

132 **2 Materials and methods**

133 *2.1 Materials*

134 CNF in the form of an aqueous suspension was kindly provided by Stora Enso AB (Sweden).
135 The CNF was produced from softwood pulp (*ca.* 75% of pine and 25% of spruce, containing 85%
136 of cellulose, 15% of hemicellulose, and traces of lignin, as determined by the supplier). CCNF, also
137 in the form of an aqueous suspension, was kindly provided by RISE Bioeconomy (Sweden). The
138 CCNF was produced from a softwood sulphite dissolving pulp (Domsjö Dissolving plus, Domsjö
139 Fabriker AB, Sweden) by carboxymethylation, as described previously (Wågberg et al., 2008),
140 followed by mechanical fibrillation. CNC in powder form was purchased from CelluForce
141 (Canada). It was produced from bleached kraft pulp by sulfuric acid hydrolysis. Charge densities of
142 -20.7 ± 0.6 , -151 ± 2 and -259 ± 4 $\mu\text{eq/g}$ at pH 5.2 were measured for CNF, CCNF and CNC,
143 respectively, using a particle charge detector PCD-02 (Mütek Analytic GmbH, Germany), titrated
144 using poly(diallyldimethylammonium chloride). Tetrabutylammonium hydroxide (TBAOH) as a 20
145 wt % aqueous solution and calcium chloride ($\geq 96.0\%$) were purchased from Sigma-Aldrich,
146 Sweden.

147 Cotton canvas with a basis weight of 417 ± 3 g/m^2 and a plain weave was obtained from Barna
148 Art (Barcelona, Spain). Dry animal glue from Lienzos Levante (Spain) was used as a sizing agent or
149 as a consolidant. Lefranc & Bourgeois® Gesso acrylic-based medium with titanium dioxide,
150 calcium carbonate and potassium hydroxide was used as a primer. Titanium White Rutile acrylic
151 paint from Vallejo® (Acrylic artist colour. Extra fine quality acrylic, ref 303), Cadmium Red
152 Medium acrylic paint from Vallejo® (Acrylic artist color. Extra fine quality acrylic, ref 805) and
153 Liquitex® professional gloss varnish were used to prepare the painted canvas samples. A cellulose

154 ether (hydroxypropyl cellulose) Klucel® G, an acrylic resin Paraloid® B72 and Beva Original
155 Formula® 371 Film lining were products from CTS Spain.

156 2.2 *Samples of painted canvas and real paintings*

157 The cotton canvas was washed by soaking overnight in a water bath. It was then dried and
158 mounted onto a stretcher. One layer of animal glue at 9.6 w/v% and *ca.* 60 °C was applied on the
159 canvas with a brush. Then, two layers of primer were applied with a plastic serigraphy squeegee in
160 cross directions. After that, two thin paint layers were applied using a soft foam roller in cross
161 directions. Finally, one varnish layer was applied using a flat soft brush. All the layers were let dry
162 several weeks before applying the next one.

163 The real painting used in this study was about 15 years old and had an acrylic paint layer on a
164 modern commercially prepared cotton canvas. It had very thin and flexible preparation and paint
165 layers on a thin canvas too.

166 2.3 *Canvas accelerated ageing*

167 A model of the degraded canvas was prepared as reported previously (Nechporchuk, Kolman,
168 et al., 2017). In brief, the method consists of treating pristine cotton canvas (70 × 80 mm) with a
169 mixture of 200 mL hydrogen peroxide solution (35 wt%) and 10 mL sulfuric acid during 72 hours
170 at 40 °C. As a result, the cellulose degree of polymerization (DP) decreased from *ca.* 6250 to *ca.*
171 450 and the breaking force for a 10 mm wide canvas stripe was reduced from 176 ± 8 N to 42 ± 4 N
172 (Nechporchuk, Kolman, et al., 2017). The canvas basis weight was reduced to 374 ± 3 g/m².

173 2.4 *Application of nanocellulose consolidation treatments*

174 In order to achieve similar viscosity, aqueous suspensions of CNF, CCFN and CNC were
175 prepared by dilution with deionized water at concentrations of 1.00, 0.25 and 3.00 wt.%,
176 respectively, and then homogenized using a Heidolph DIAX 900 (Heidolph Instruments, Germany)
177 equipped with a 10 F shaft at power 2 (around 11,600 rpm). These suspensions were
178 homogeneously spread on the surface of the aged cotton canvas samples (70 × 80 mm) using a
179 plastic serigraphy squeegee. The coatings were deposited in 1–3 passes with an interval of 20 min
180 to allow some water to evaporate. Table 1 shows the increase of the canvas basis weight after
181 coating, measured by gravimetry. After drying, one batch of CCFN canvas samples, with different
182 amount of deposited nanocellulose, was treated with a 0.5 M CaCl₂ aqueous solution (*ca.* 2 g of
183 solution per m²) to cross-link the nanofibrils (Dong, Snyder, Williams, & Andzelm, 2013), which
184 was applied by spraying with a Cotech Airbrush Compressor AS18B (Clas Ohlson AB, Sweden) at
185 a pressure of 2 bar. One batch of samples was prepared by mixing CCFN suspensions with TBAOH
186 (5/1 wt/wt dry) to reduce the hydrophilicity of the cellulose (Shimizu, Saito, Fukuzumi, & Isogai,
187 2014).

188

189 **Table 1** List of treatments used for aged canvas consolidation and the basis weight uptake after the coating.

Sample name	Description	Basis weight uptake (%) with number of coatings		
		1	2	3
CNF	Canvas coated with cellulose nanofibril suspension at 1 wt.%	2.5	5.0	7.2
CCNF	Canvas coated with carboxymethylated cellulose nanofibril suspension at 0.25 wt.%	0.6	1.2	1.8
CNC	Canvas coated with cellulose nanocrystal suspension at 3 wt.%	7.4	14.8	22.2

190

191 *2.5 Application of conventional consolidants*

192 Three different adhesives, animal glue, Klucel G and Paraloid B72, which have been
 193 traditionally used to consolidate painting canvases, were applied on the aged cotton canvas as
 194 shown in Table 2. A lining of the aged canvas using a Beva 371 film and a new linen canvas was
 195 also performed. The canvas was fixed on a flat rigid surface along the borders to avoid shrinkage
 196 during the treatment. When brushing, a flat 4 cm wide brush was used. When using an airbrush,
 197 samples were set in an upright position and applications were performed from a distance of 10 cm
 198 to cover the canvas homogeneously in horizontal and vertical directions. A limited amount of
 199 consolidant was applied during spraying to avoid flooding the canvas, which is important in order
 200 to avoid canvas shrinkage. Coatings were left to dry for 5–10 minutes between applications. Profi-
 201 AirBrush Compact II airbrush was used, with a 0.3 mm needle, consolidant gravity feed and 2.5 bar
 202 pressure.

203

204 **Table 2** List of traditional consolidants applied on the aged canvases

Sample name	Concentration and solvent	Application system and number of coatings
Animal Glue	5 w/v% in water	Brush, 1 coating, soaking the canvas
Klucel® G	1 w/v% in ethanol	Airbrush, 4 coatings without soaking the canvas
Paraloid® B72	5 w/v% in acetone	Airbrush, 1 coating without soaking the canvas
		Brush, 1 coating, soaking the canvas
Beva Original Formula® 371 Film (lining)	Film	Lining onto a new linen canvas. Beva film first attached to the lining canvas, then to the cotton sample with a hot spatula at 65°C

205

206 *2.6 Tensile testing*

207 Mechanical testing was carried out according to the ASTM D5034 – 09 method (“ASTM D5034
 208 – 09 (2013) Standard Test Method for Breaking Strength and Elongation of Textile Fabrics (Grab
 209 Test),” 2013) with slight deviations. The measurements were performed using Instron 5565A
 210 (Norwood, MA, USA) equipped with a static load cell of 100 or 5000 N and pneumatic clamps
 211 operated at a pressure of 5 bar. Rectangular specimens with a length of 70 mm and a width of
 212 10 mm were cut parallel to the warp or the weft direction along the threads. The samples were

213 conditioned at least 12 h before the measurements at a relative humidity (RH) of 60% and a
214 temperature of 23 °C. Sandpaper was used between the canvas sample and the clamps (with the
215 grains facing the canvas) to avoid slippage. The measurements were carried out at a constant
216 extension rate of 300 mm/min and a gauge length of 20 mm. The force was measured as a function
217 of elongation and then expressed in Newtons per meter of canvas length (Berger & Russell, 1988) .
218 Seven measurements were performed for each specimen and the average values were then
219 calculated. A digital video camera operating at 30 frames per second was used for video recording
220 during the tensile testing of the samples of painted canvas and real painting in order to detect the
221 point where the cracking became visible.

222 *2.7 Atomic force microscopy (AFM)*

223 AFM was performed in tapping mode using NTEGRA Prima equipped with a NSG01 cantilever
224 (NT-MDT, Russia) to examine the morphology of the nanocellulose samples. For sample
225 preparation, the CNF/CCNF and the CNC suspensions were diluted to a concentration of 10^{-2} and
226 10^{-3} wt.%, respectively, and a droplet of each suspension was placed on a freshly cleaned silicon
227 wafer substrate and dried. The AFM height images were then processed with the Gwyddion
228 software. The nanoparticle diameter was determined from the height profiles of AFM height images
229 as an average of 100 measurements.

230 *2.8 Scanning electron microscopy (SEM)*

231 The cross-section of the coated canvases was analyzed using Leo Ultra 55 field emission gun
232 (FEG) SEM (Carl Zeiss SMT GmbH, Germany). The SEM was operated at an acceleration voltage
233 of 3 kV. The canvas cross-section was prepared by clear cut with a new razor blade punched with a
234 hammer. The samples were mounted onto stubs and sputtered with a gold layer of *ca.* 10 nm using a
235 Sputter Coater S150B (Edwards, UK).

236 *2.9 Controlled relative humidity dynamic mechanical analysis (DMA-RH)*

237 Dynamic mechanical analysis was carried out using a Tritec 2000 B (Lacerta Technology Ltd.,
238 UK) equipped with a humidity controller. The samples were cut in warp direction with a width of
239 10 threads and a gauge length of 5 mm. The measurements were carried out at a frequency of 1 Hz,
240 an amplitude of 0.1% of strain and a temperature of 25 °C. The samples were subjected to ramps in
241 the region of 20–60 %RH at a rate of 4 %RH/min with an equilibration at each RH of 30 min. Three
242 RH cycles (20–60%RH) were performed for each sample.

243

244 **3 Results and Discussion**

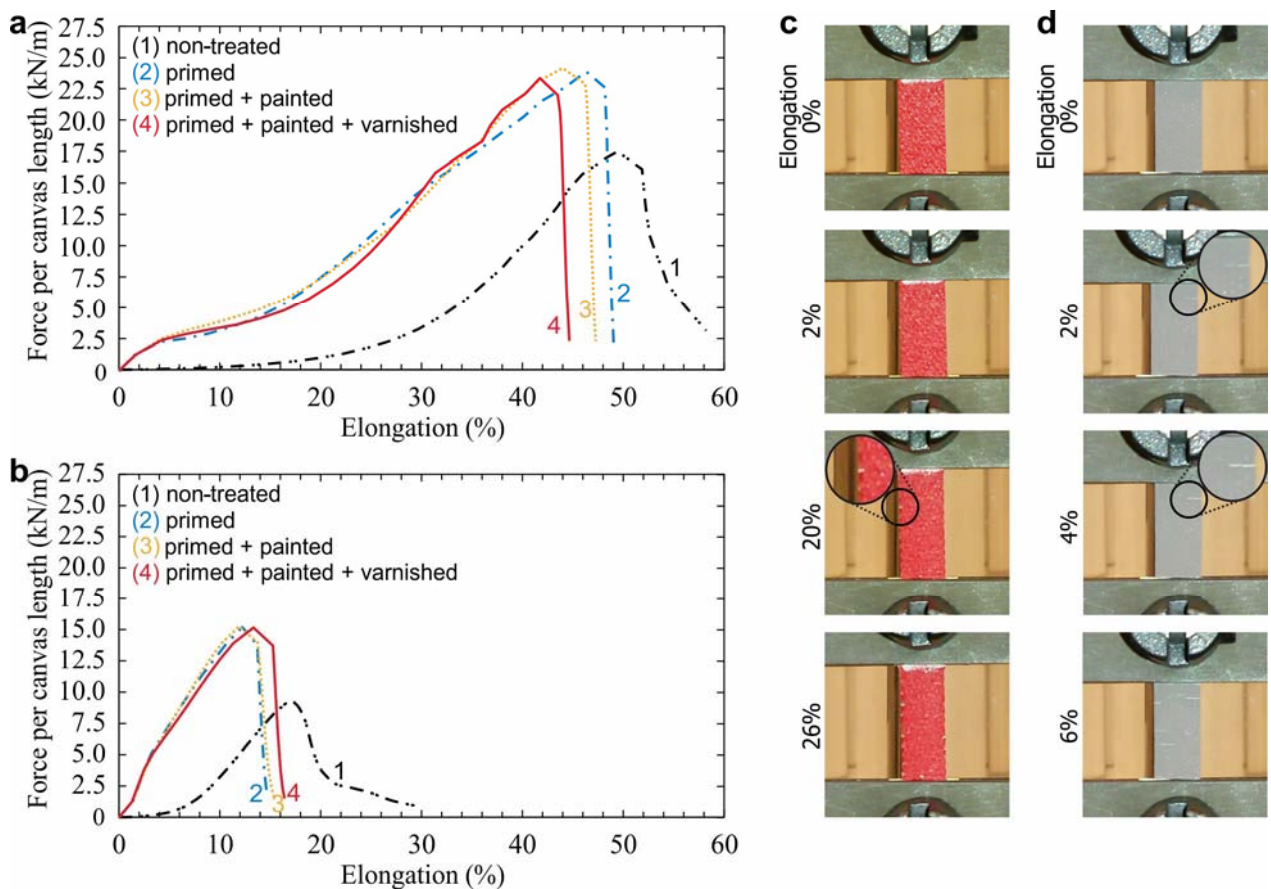
245 *3.1 Mechanical properties of canvas paintings*

246 In order to provide a rational reinforcement of the degraded canvases, it was necessary to
247 determine the elongation regime where the reinforcement should be provided, *i.e.*, to specify

248 whether the initial stretchable character of the canvas should be reproduced or if the consolidation
 249 treatment should stiffen the canvas. New cotton canvas was coated with prime, paint and varnish,
 250 and was examined after each layer deposition in both warp and weft directions using tensile testing.

251 The force-elongation curves both in warp and weft directions are shown in Fig. 1a and b,
 252 respectively. The measurements revealed an increase of the breaking force and a slight reduction of
 253 elongation at break in both directions when the canvas was primed. The values went from
 254 17.6 ± 0.8 kN/m to 24.0 ± 1.4 kN/m for the breaking force and from $52.7 \pm 1.1\%$ to $48.9 \pm 2.7\%$ for
 255 the elongation at break in warp direction. A sharp increase of the slope of the curve in low
 256 elongation regime after priming indicates its stiffening effect. Taking into account an increase of
 257 canvas thickness from 0.814 mm to 0.948 mm as a result of the priming, and applying the reduction
 258 factor of 25% for the canvas cross-section (area of the threads parallel to the force direction)
 259 (Mecklenburg, McCormick-Goodhart, & Tumosa, 1994), the Young's modulus in the linear domain
 260 of elongation ($<2\%$) in the warp direction was quantified as 17.6 ± 0.8 MPa and 356.0 ± 18.0 MPa
 261 for the original and the primed canvas, respectively. The subsequent application of paint and
 262 varnish, which were both much thinner than the prime layer, did not significantly affect the
 263 mechanical behavior.

264



265
 266 **Fig. 1.** Mechanical properties of new cotton canvas treated with prime, paint and varnish layers, measured in (a) warp
 267 and (b) weft directions. Images of the primed and painted new canvas (c) and real painting (d), both captured during
 268 tensile testing at various elongations, measured in warp direction. The circles in c and d show crack propagation.

269

270 The linear region of deformation of the painted canvases was found to be quite short (<2%
271 elongation). Outside this region the deformation is known to be irreversible (Stachurski, 1997) and
272 the paint layer is likely to deteriorate. Therefore, the consolidation treatment should provide
273 substantial reinforcement in this region to prevent paint cracking. The samples that were primed and
274 painted were first examined visually to detect possible cracks. On Fig. 1c, which relates to a freshly
275 made painting, the propagation of cracks became noticeable only at *ca.* 20% elongation. In
276 comparison, for the real painting samples shown in Fig. 1d, the paint layer started to crack already
277 at 2% elongation. The increased brittleness of aged paintings is a known phenomenon and is due to
278 chemical changes, such as gradually increasing degree of crosslinking and loss of plasticizer
279 (Michalski, 1991). Prevention of this process is crucial; otherwise, it will eventually lead to flaking
280 and to the deterioration of the paint layer. Such a low elongation regime for paint cracking
281 suggested that the consolidation treatment should provide a stiff support at low elongation in order
282 to prevent paint cracking, which was also suggested previously (Berger & Russell, 1988).

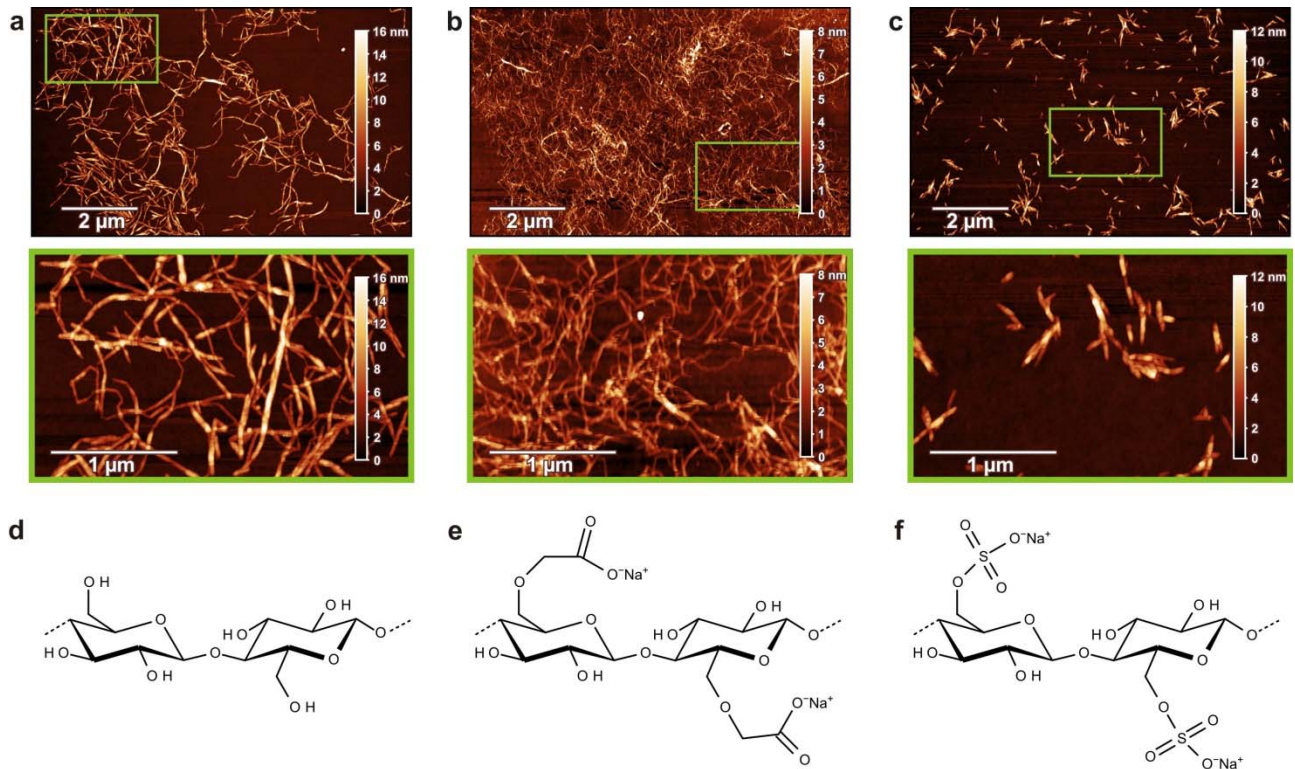
283

284 3.2 Consolidation of aged canvas with nanocellulose: morphological characterization

285 The reinforcement potential of the different nanocellulose samples, *viz.*, CNF, CCNF and CNC,
286 was analyzed in this study as an alternative to conventional consolidation practices. The
287 nanocellulose formulations were examined on a model of degraded cotton canvas developed
288 previously (Nechyporchuk, Kolman, et al., 2017). The morphology of these nanocelluloses is
289 shown in Fig. 2a–c. CNF (Fig. 2a) had a thickness of 7.0 ± 2.8 nm and a length of several
290 micrometers. CNC (Fig. 2c) had similar diameter, 7.5 ± 2.8 nm, but was smaller in length, *ca.*
291 0.5 μ m. Finally, CCNF (Fig. 2b) was much thinner compared to the others, 2.4 ± 0.9 nm, and had a
292 length of several micrometers.

293 Simplified surface chemical structures of CNF, CCNF and CNC are shown in Fig. 2d, e and f,
294 respectively. These nanocellulose samples were extracted from wood using different processing
295 routes, including surface functionalization for CCNF and CNC. Carboxymethyl and sulfate ester
296 groups resulted in the presence of negative charges on the surface at basic and neutral pH (charge
297 densities are shown in the Materials and Methods section). This introduced repulsive interactions
298 between the nanofibers and gave better dispersibility, which may enhance the penetration into the
299 canvas. The dimensional and surface charge differences among the nanocelluloses may influence
300 the film-forming properties on canvases and the final mechanical properties of the coated canvases.
301 Additionally, CCNF and CNC can exhibit acidic character, as the pKa of the functional groups is
302 below 7, which should be considered for achieving long-term stability of the consolidation
303 treatment. However, when deacidification of the canvas is performed and a certain alkaline reserve

304 is present (Giorgi et al., 2002), its buffering activity may avoid the acidity issue. This question
305 remains beyond the present work and requires further investigation.
306

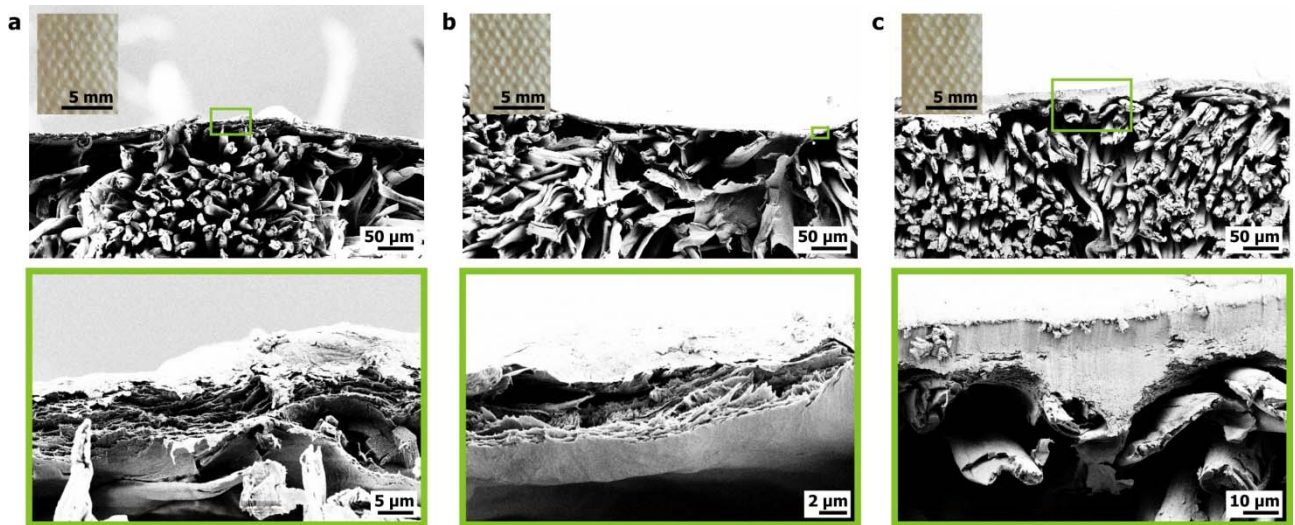


307
308 **Fig. 2.** Atomic force microscopy images (a, b, c) and the corresponding simplified surface chemistries (d, e, f) of: (a, d)
309 mechanically isolated cellulose nanofibrils (CNF); (b, e) carboxymethylated cellulose nanofibrils (CCNF) and (c, f)
310 cellulose nanocrystals (CNC). The color gradient bars shown in the AFM images represent the height scale, also
311 referred to as the thickness.

312
313 Fig. 3a, b and c show SEM images of cross-sections for the canvas samples coated with 3 layers
314 of CNF, CCNF and CNC, respectively. From the upper SEM images, the nanocellulose coatings are
315 barely seen. Instead, the canvas structure, consisting of microscopic fibers, is clearly visible. It is
316 seen that none of the nanocelluloses penetrated much into the canvas bulk, instead, forming a film
317 on the canvas surface. It is interesting that this was the case also for CNC, which, as discussed
318 above, consists of short nanoparticles that unlike CNF do not form highly entangled flocs
319 (Nechporchuk, Pignon, & Belgacem, 2015). One may anticipate large flocs present in CNF to be
320 trapped by the canvas fibers and, therefore, not penetrate much into the porous material. However,
321 it is obvious that a non-flocculated suspensions of charged CCNF and CNC also resist penetration.
322 Similar film-forming properties have been observed previously when coating textiles with CNF
323 (Nechporchuk, Yu, Nierstrasz, & Bordes, 2017).

324 We assume that the poor penetration is related to fast water absorption by canvas fibers from the
325 nanocellulose suspensions, which leads to increased viscosity of the suspensions and arrested flow
326 into the canvas depth. Application of further coating layers leads to a better-developed continuous

327 film on the canvas surface. Such good film-forming properties on the canvas surface without
328 noticeable penetration have a good potential to result in reversible consolidation treatment, which
329 can be further removed from the surface, if necessary.
330



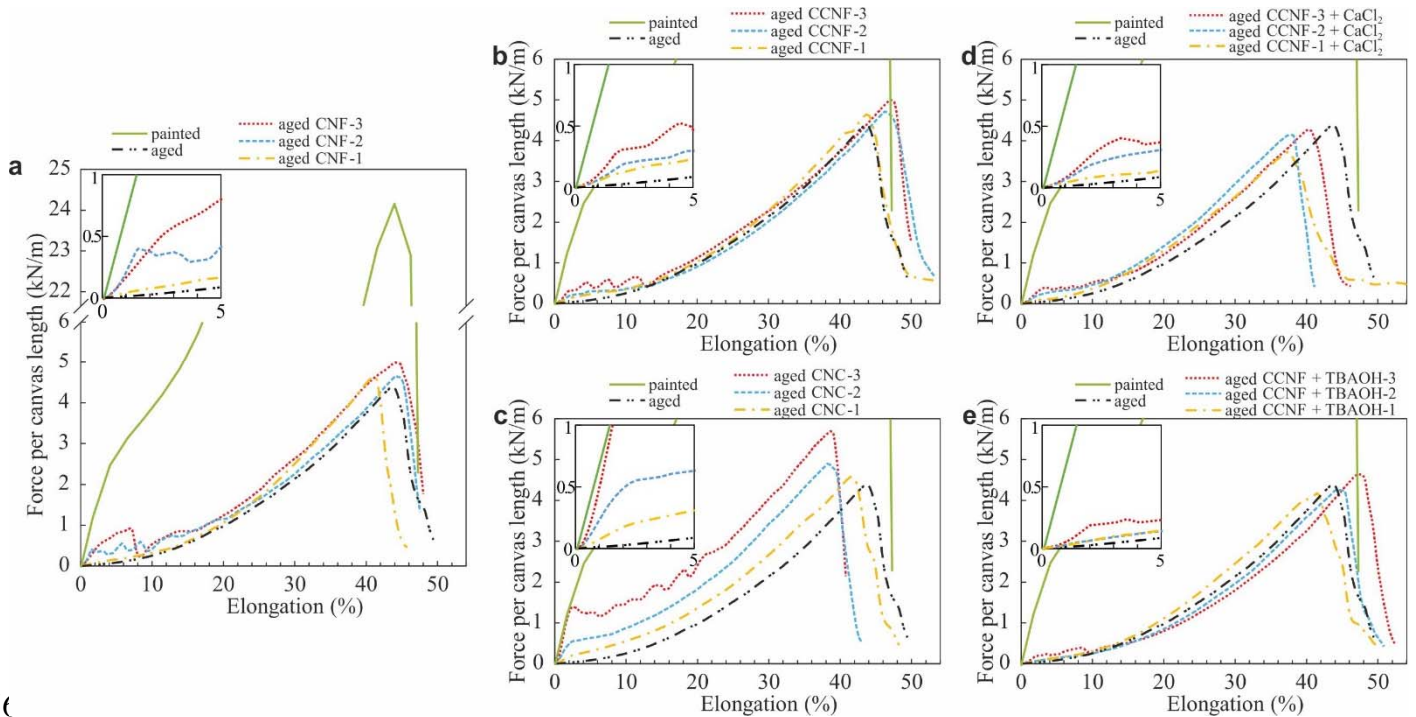
331
332 **Fig. 3.** Scanning electron microscopy images of aged cotton canvases coated 3 times with: (a) CNF; (b) CCNF and (c)
333 CNC, with optical microscopy images as insets (left top).

334
335 It was also observed that CNF and CCNF formed highly porous films with lamellar self-
336 assembled structure (see Fig. 3a, b). Similar structures have been previously reported for self-
337 standing CNF films prepared by different methods (Henriksson, Berglund, Isaksson, Lindström, &
338 Nishino, 2008; Li et al., 2016) and for CNF coatings on fabrics (Nechyporchuk, Yu, Nierstrasz, &
339 Bordes, 2017). CNC tended to form more dense structures (see Fig. 3c) due to better packing
340 capacity of rod-like nanoparticles, compared to the flexible nanofibrils. Additionally, the insets (top
341 left) in Fig. 3a, b and c show that such nanocellulose films do not distinctly change the visual
342 appearance of the canvases, which is in line with the minimal intervention principle of canvas
343 restoration (Ackroyd et al., 2002), especially compared to lining with a new canvas.

344 345 *3.3 Mechanical properties of the consolidated aged canvases*

346 Fig. 4 shows force-elongation curves for model aged canvases coated with different
347 nanocellulose-based formulations measured in warp direction. Mechanical properties of the painted
348 pristine canvas are also given as reference. The canvases with one, two or three coatings with a
349 given consolidation formulation are shown, as well as the bare degraded canvas. The curve
350 representing an average of seven measurements for each sample is plotted. The mechanical
351 properties in low elongation regime are the most important here, as discussed previously, and are
352 shown in insets. However, we also present the whole curves in order to compare the performance of

353 nanocellulose treatments further with conventional consolidants, since some of them provide more
 354 distinct features in the whole elongation range.
 355



356
 357 **Fig. 4.** Mechanical properties of the aged canvases coated with different number of coatings of: (a) CNF, (b) CCNF, (c)
 358 CNC, (d) CCNF + CaCl₂ and (e) CCNF + TBAOH. The curves for painted new canvas are also shown.

359
 360 As can be seen from Fig. 4a, the slope of the tensile curves enhanced drastically in the low
 361 elongation region (< 5%) by applying CNF, see Fig. 4a, indicating the increase of stiffness. Since
 362 the coatings did not much influence the canvas thickness, this led to an increase of Young's
 363 modulus. The larger the number of coatings on the canvas, the larger the increase of the modulus.
 364 The use of CNF gave an increased force over the entire elongation range and increased the breaking
 365 force. In the elongation range of 5–10%, some fluctuations of the force were observed, which can
 366 be attributed to cracking of the nanocellulose coating. In this case, the periodic decrease of the
 367 measured force occurred due to inertia created after breakage of the coating.

368 The inset in Fig. 4a demonstrates better the low elongation regime of the canvas coated with
 369 CNF. The CNF consolidation with 3 layers exhibits linear (reversible) deformation up to ca.
 370 500 N/m at an elongation of up to 3%, which exceeds the maximum sustainable tension of 200–
 371 300 N/m above which an average painting canvas is torn (Berger & Russell, 1990; Iaccarino
 372 Idelson, 2009; Roche, 1993). Even though the curve had a lower slope than a painted new canvas,
 373 the improved stiffness compared with that of the aged canvas was significant. The coating with 2
 374 CNF layers can be considered as an acceptable level of consolidation as well. Such stiffening effect
 375 is well in line with previous studies (Völkel et al., 2017; Nechporchuk, Yu, et al., 2017).

376 The use of CCNF resulted in a smaller increase of the stiffness, as compared to CNF. This
377 occurred since a lower concentration of nanocellulose was used in the case of CCNF suspension,
378 resulting in lower dry weight increase of the coating (see Table 1). A lower concentration was used
379 because of the higher nanofibril aspect ratio of CCNF, which led to more viscous gels at equivalent
380 concentrations (Nechyporchuk, Belgacem, & Pignon, 2016). With CCNF as coating material, the
381 canvas exhibited not only a higher breaking force compared to neat canvas, it gave higher
382 elongation at break as well, which is probably also related to the higher nanofibril aspect ratio.
383 Three coatings with CCNF, which in terms of mass gain is close to one coating with CNF, yielded a
384 higher curve slope than the canvas coated with one layer of CNF, suggesting that a higher level of
385 reinforcement can be achieved with the same deposited dry weight of coating.

386 CNC coatings provided the lowest level of reinforcement normalized by the deposited weight,
387 which can be explained by the fact that they possess the lowest aspect ratio. On the other hand, the
388 possibility of coating with a suspension of higher concentration resulted in better reinforcement
389 compared to the others when three coating layers were deposited. When using CNC, both Young's
390 modulus and the breaking force increased, while the elongation at break was reduced. The
391 mechanical behavior of the coated canvas with 3 layers of CNC in the low elongation regime (up to
392 3%) matched perfectly the behavior of newly painted canvas, thus suggesting that such level of
393 reinforcement can well support the paint layer, see inset in Fig. 4c. The coating with 2 layers of
394 CNC also provided an acceptable level of reinforcement.

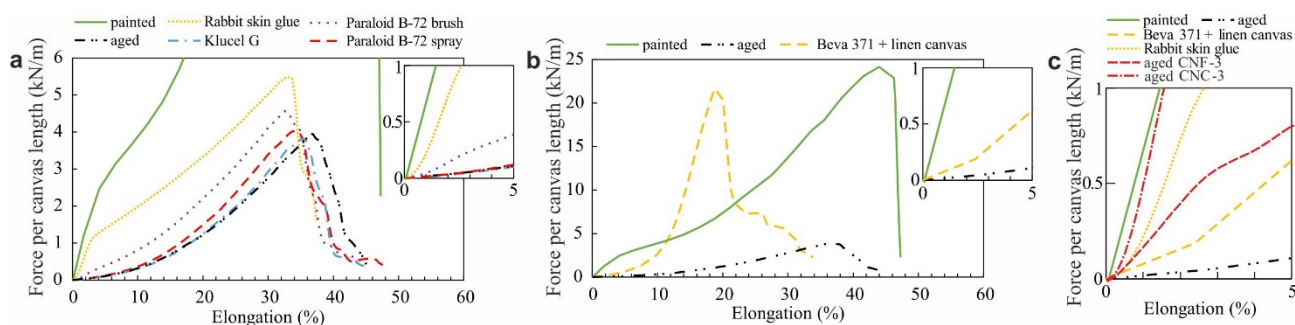
395 Attempts to improve the mechanical properties of CCNF by ionic cross-linking or to reduce its
396 sensitivity to water by hydrophobization with TBAOH did not give major improvements, as shown
397 in Fig. 4d and e.

398 The nanocellulose suspensions used are all aqueous, which means that each application
399 introduces water into the canvas, which is then evaporated. These events should be minimized in
400 order to prevent dimensional variations of the canvas due to swelling and shrinkage. Therefore, the
401 canvas consolidation treatment will be a compromise between the highest possible reinforcement,
402 the lowest mass uptake (which are both best provided by CCNF) and the lowest water content in the
403 suspension (best provided by CNC). CNF is in-between CCNF and CNC in these regards. The
404 suspensions were manipulated in this work at concentrations that allowed them to be sprayed on the
405 canvas using an airbrush. This may reduce the amount of water exposed to the canvas due to
406 enhanced evaporation during spraying. No distinct difference in the extent of nanocellulose
407 penetration into the canvas was observed when comparing spraying and application using a brush.

408 The newly developed consolidation treatments can be seen as an alternative to the conventional
409 ones. Therefore, the mechanical properties of the model aged cotton canvases treated with some
410 traditional restoration materials were studied and compared with the values obtained with the

411 nanocellulose coatings. Fig. 5a shows that Klucel G (hydroxypropyl cellulose), a popular leather
 412 and paper consolidant, reduced slightly the elongation at break without affecting much Young's
 413 modulus and the breaking force. Therefore, at that deposited quantity, it did not provide proper
 414 canvas reinforcement. Similar behavior was observed for sprayed Paraloid B-72 (acrylic resin).
 415 When the same formulation was applied by brush, a distinct improvement of the mechanical
 416 properties was observed, however. There was an increase in both Young's modulus and the
 417 breaking force. Finally, the use of rabbit skin glue resulted in a strong enhancement of both stiffness
 418 and strength.

419



420

421 **Fig. 5.** Mechanical properties of aged canvases after various consolidation treatments

422

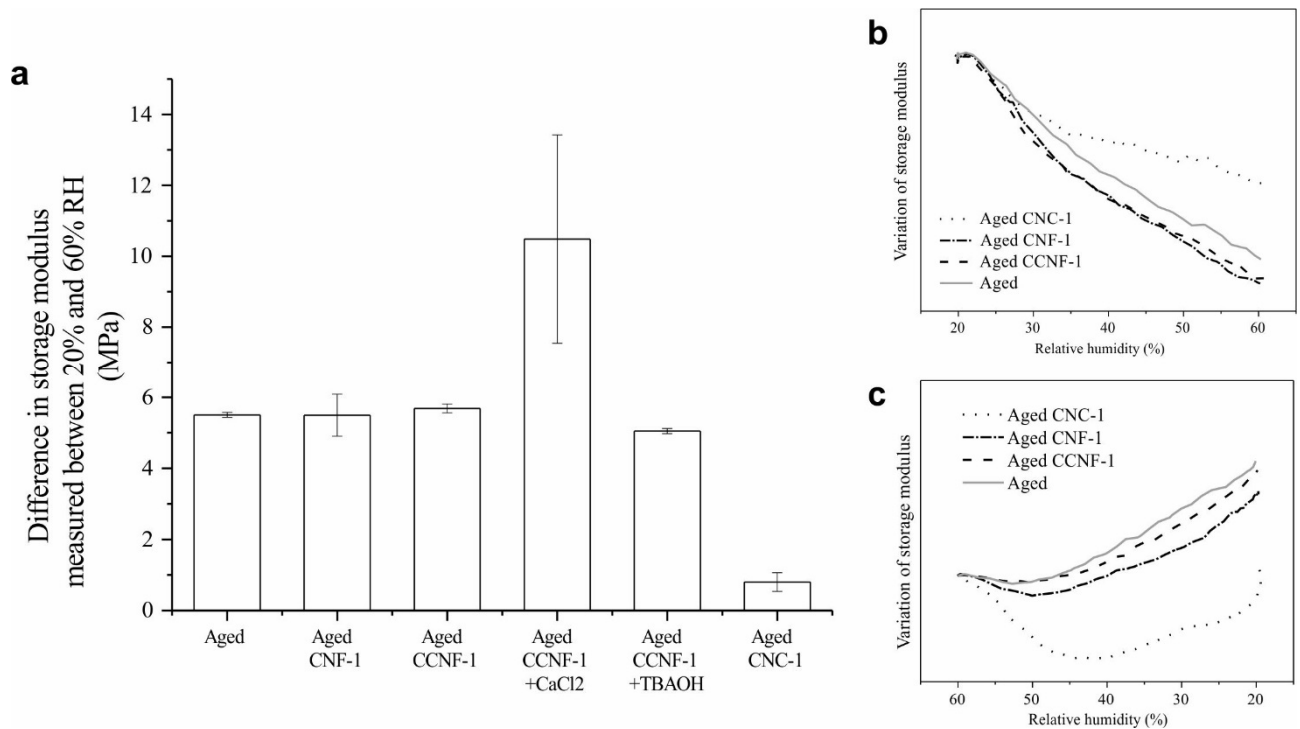
423 Fig. 5b shows the mechanical properties of the aged canvas coated with Beva Original Formula®
 424 371 Film and lined with a linen canvas. The strength of the consolidated canvas almost reached the
 425 value of the newly painted canvas. However, the stiffness was not increased much in the low
 426 elongation region; thus, the treatment did not provide a stiff support for the paint. In the range
 427 usually used to stretch paintings (0 N/m to 300 N/m and 0% to 3% elongation) among all the
 428 materials shown in Fig. 5 only the animal glue reinforced the canvas in a proper way. On the other
 429 hand, deposition of animal glue is known to cause strong contraction of the canvas upon drying
 430 (Ackroyd, 2002). Fig. 5c provides direct comparison of the best performing traditional consolidants
 431 with nanocellulose coatings (3 layers) in low elongation region. Compared to the conventional
 432 consolidants, CNC showed the highest level of consolidation. Both CNC and CNF provided better
 433 reinforcement than conventional lining with Beva Original Formula® 371 Film and linen canvas.

434

435 *3.4 Influence of relative humidity (RH) variations on the mechanical stability of the consolidated* 436 *canvases*

437 In order to confirm the suitability of nanocelluloses as an alternative to traditional consolidants,
 438 it is important to assess the influence of variations in RH on the mechanical properties of the treated
 439 models of degraded canvas. DMA-RH has been used previously to evaluate effects of
 440 environmental conditions and preventive conservation treatment on painting canvases (Foster,

441 Odlyha, & Hackney, 1997). Variations in RH can influence the dimensional stability of the canvas
 442 and a nanocellulose layer responding too strongly to environmental changes would be detrimental.
 443 Fig. 6a shows the variation of storage modulus (E') between two relative humidity levels measured
 444 with DMA-RH on the 2nd cycle. The humidification and dehumidification profiles are shown
 445 separately in Fig. 6b and c, respectively. It can be seen that the response to RH variations for coated
 446 and uncoated samples was similar: all the samples exhibited higher stiffness at low RH (20%) and
 447 lower stiffness at high RH (60%). This effect can be explained by a plasticizing action of water
 448 molecules on the cellulosic chains. An increased water content will lead to reduced intermolecular
 449 cellulose interactions through hydrogen bonding.
 450



451
 452 **Fig. 6.** Variation of the storage modulus of consolidated aged canvases applying different relative humidity levels (a),
 453 including humidification (b) and dehumidification (c) profiles.

454
 455 The variation of E' was similar for the aged canvas and the one coated with CNF and CCNF
 456 (Fig. 6a). The smallest differences in stiffness at the RH plateaus were observed for CNC despite
 457 this material having highly hydrophilic sulfate groups (see Fig. 2f) on the surface. This may be
 458 explained by the higher density of the CNC coatings as compared to the coatings with CNF and
 459 CCNF, as shown previously in Fig. 3. The use of calcium chloride for ionic cross-linking of the
 460 CCNF coating resulted in a much enhanced variation of E' . Most likely, this is due to the excess of
 461 salt that was introduced. Free salt in the material will make it more responsive towards moisture
 462 changes. These results demonstrate the difficulties of such a cross-linking approach. Finally, the use

463 of TBAOH did not much influence the stiffness variations, although one may expect that the
464 TBAOH treatment will induce hydrophobicity to the coating.

465 Analysis of the transition regions of RH (humidification and dehumidification) revealed that
466 during the moistening (see Fig. 6b) the canvas coated with CNC had the lowest decrease of E' .
467 However, during the dehumidification (see Fig. 6c), the CNC-coated canvas exhibited a strong
468 decrease followed by an increase of the storage modulus, which was not so pronounced or even
469 absent in all the other samples. From these results, it seems that before reaching a certain steady
470 state, the canvas might have to experience several RH cycles, which would in practice be achieved
471 in the early lifetime of the treatment. The reasons behind such behavior are complex, and it could be
472 that an equilibrium in terms of moisture diffusion through the nanocellulose layer and the canvas
473 has to be reached.

474

475 **4 Conclusions**

476 Canvas degradation is one of the crucial issues of easel paintings, which leads to their irreversible
477 damage. In this work, we demonstrate for the first time that different types of natural cellulose
478 nanomaterials have a potential for use as a mechanical reinforcement of degraded cellulosic canvases.
479 Such treatments are also in line with the strategy of minimal intervention. The results show that
480 nanocellulose can provide a substantial reinforcement in the low elongation region, *i.e.* below 3%,
481 that is where strengthening should be provided. In this region, the stiffening effect of CNF, CCFN
482 and CNC is much higher than that achieved using traditional wax-resin formulation (Beva 371).
483 Despite the high porosity of the canvas, nanocellulose, irrespectively of the aspect ratio of the
484 nanofibers, formed a film after deposition from a diluted suspension. The structure of the reinforcing
485 film was markedly influenced by the aspect ratio of the nanocelluloses — short CNC formed a dense
486 homogeneous layer, while longer CNF and CCFN yielded layered structures.

487 When comparing different types of nanocellulose, CCFN showed better performance per gained
488 weight. However, it could only be handled at a low solids content, which means that the canvas was
489 exposed to larger water volumes than with the other nanocelluloses. Attempts to reduce the sensitivity
490 of CCFN to water by ionic cross-linking and by hydrophobization did not exhibit major
491 improvements. CNC showed the smallest reinforcement per gained weight but the highest
492 reinforcement per equivalent number of coatings, due to the possibility to use higher solids content
493 in the aqueous dispersion. Moreover, CNC gave the lowest mechanical changes upon RH variations,
494 which can be beneficial for further preservation of canvas upon storage. CNF compromised the mass
495 uptake and the mechanical reinforcement and did not change the responsiveness of the treated canvas
496 to humidity variations. Unlike CCFN and CNC, CNF does not carry acidic chemical groups and
497 therefore has a potential to have better long-term stability. On the other hand, when deacidification

498 of the canvas is performed and a certain alkaline reserve is present, this acidic character of CCNF and
499 CNC may not induce any problems. Acidity remains beyond the scope of this work and should be
500 addressed by further research. Additionally, the dimensional changes of the canvas upon wetting and
501 drying affected by deposition of nanocellulose suspensions should be studied.

502 Nanocellulose is similar in nature to cotton and is an attractive alternative to the synthetic polymers
503 used today for canvas consolidation. Some of the other advantages are: no alteration of canvas color
504 and low depth of impregnation Nanocellulose also has higher degree of crystallinity compared to
505 canvas fibers, which may be a key towards long-term stability. Another crucial aspect is the
506 reversibility of the treatment. The good film forming properties of the nanocelluloses on the surface
507 of the canvas mean that there is limited penetration into the bulk of the canvas, thus providing
508 potential for removing it if needed at a later stage.

509

510 **Acknowledgements**

511 This work has been performed in the frame of NANORESTART (NANOmaterials for the
512 RESToration works of ART) project funded by Horizon 2020 European Union Framework Program
513 for Research and Innovation (Grant Agreement No. 646063). The authors express their gratitude to
514 RISE Bioeconomy (Sweden) and Stora Enso AB (Sweden) for providing the nanocellulose samples.

515

516 **References**

- 517 Ackroyd, P. (2002). The structural conservation of canvas paintings: changes in attitude and
518 practice since the early 1970s. *Studies in Conservation*, 47(sup1), 3–14.
519 <https://doi.org/10.1179/sic.2002.47.Supplement-1.3>
- 520 Ackroyd, P., Phenix, A., & Villers, C. (2002). Not lining in the twenty-first century: Attitudes to the
521 structural conservation of canvas paintings. *The Conservator*, 26(1), 14–23.
522 <https://doi.org/10.1080/01410096.2002.9995172>
- 523 ASTM D5034 – 09 (2013) Standard Test Method for Breaking Strength and Elongation of Textile
524 Fabrics (Grab Test). (2013).
- 525 Berger, G. A. (1972). Formulating Adhesives for the Conservation of Paintings. *Studies in*
526 *Conservation*, 17(sup1), 613–629. <https://doi.org/10.1179/sic.1972.17.s1.011i>

- 527 Berger, G. A., & Russell, W. H. (1988). An evaluation of the preparation of canvas paintings using
528 stress measurements. *Studies in Conservation*, 33(4), 187–204.
529 <https://doi.org/10.1179/sic.1988.33.4.187>
- 530 Berger, G. A., & Russell, W. H. (1990). Deterioration of Surfaces Exposed to Environmental
531 Changes. *Journal of the American Institute for Conservation*, 29(1), 45–76.
532 <https://doi.org/10.1179/019713690806046145>
- 533 Bianco, L., Avalle, M., Scattina, A., Croveri, P., Pagliero, C., & Chiantore, O. (2015). A study on
534 reversibility of BEVA®371 in the lining of paintings. *Journal of Cultural Heritage*, 16(4),
535 479–485. <https://doi.org/10.1016/j.culher.2014.09.001>
- 536 Chelazzi, D., Chevalier, A., Pizzorusso, G., Giorgi, R., Menu, M., & Baglioni, P. (2014).
537 Characterization and degradation of poly(vinyl acetate)-based adhesives for canvas
538 paintings. *Polymer Degradation and Stability*, 107, 314–320.
539 <https://doi.org/10.1016/j.polymdegradstab.2013.12.028>
- 540 Dong, H., Snyder, J. F., Williams, K. S., & Andzelm, J. W. (2013). Cation-Induced Hydrogels of
541 Cellulose Nanofibrils with Tunable Moduli. *Biomacromolecules*, 14(9), 3338–3345.
542 <https://doi.org/10.1021/bm400993f>
- 543 Dreyfuss-Deseigne, R. (2017). Nanocellulose Films in Art Conservation. *Journal of Paper*
544 *Conservation*, 18(1), 18–29. <https://doi.org/10.1080/18680860.2017.1334422>
- 545 Foster, G., Odlyha, M., & Hackney, S. (1997). Evaluation of the effects of environmental
546 conditions and preventive conservation treatment on painting canvases. *Thermochimica*
547 *Acta*, 294(1), 81–89. [https://doi.org/10.1016/S0040-6031\(96\)03147-4](https://doi.org/10.1016/S0040-6031(96)03147-4)
- 548 Giorgi, R., Dei, L., Ceccato, M., Schettino, C., & Baglioni, P. (2002). Nanotechnologies for
549 Conservation of Cultural Heritage: Paper and Canvas Deacidification. *Langmuir*, 18(21),
550 8198–8203. <https://doi.org/10.1021/la025964d>

- 551 Habibi, Y., Lucia, L. A., & Rojas, O. J. (2010). Cellulose Nanocrystals: Chemistry, Self-Assembly,
552 and Applications. *Chemical Reviews*, *110*(6), 3479–3500.
553 <https://doi.org/10.1021/cr900339w>
- 554 Hedley, G. (1988). Relative humidity and the stress/strain response of canvas paintings: uniaxial
555 measurements of naturally aged samples. *Studies in Conservation*, *33*(3), 133–148.
556 <https://doi.org/10.1179/sic.1988.33.3.133>
- 557 Hendrickx, R., Desmarais, G., Weder, M., Ferreira, E. S. B., & Derome, D. (2016). Moisture uptake
558 and permeability of canvas paintings and their components. *Journal of Cultural Heritage*,
559 *19*, 445–453. <https://doi.org/10.1016/j.culher.2015.12.008>
- 560 Henriksson, M., Berglund, L. A., Isaksson, P., Lindström, T., & Nishino, T. (2008). Cellulose
561 Nanopaper Structures of High Toughness. *Biomacromolecules*, *9*(6), 1579–1585.
562 <https://doi.org/10.1021/bm800038n>
- 563 Iaccarino Idelson, A. (2009). About the choice of tension for canvas paintings. *CeROArt*.
564 *Conservation, Exposition, Restauration d'Objets d'Art*, *4*.
- 565 Klemm, D., Heublein, B., Fink, H.-P., & Bohn, A. (2005). Cellulose: Fascinating Biopolymer and
566 Sustainable Raw Material. *Angewandte Chemie International Edition*, *44*(22), 3358–3393.
567 <https://doi.org/10.1002/anie.200460587>
- 568 Kolman, K., Nechyporchuk, O., Persson, M., Holmberg, K., & Bordes, R. (2017). Preparation of
569 silica/polyelectrolyte complexes for textile strengthening applied to painting canvas
570 restoration. *Colloids and Surfaces A: Physicochemical and Engineering Aspects*, *532*, 420–
571 427. <https://doi.org/10.1016/j.colsurfa.2017.04.051>
- 572 Li, Q., Chen, W., Li, Y., Guo, X., Song, S., Wang, Q., ... Zeng, J. (2016). Comparative study of the
573 structure, mechanical and thermomechanical properties of cellulose nanopapers with
574 different thickness. *Cellulose*, *23*(2), 1375–1382. <https://doi.org/10.1007/s10570-016-0857->
575 6

576 Mecklenburg, M. F. (1982). Some aspects of the mechanical behavior of fabric supported paintings.
577 *National Museum Act.*

578 Mecklenburg, M. F. (2005). The structure of canvas supported paintings. In *International*
579 *conference on painting conservation: canvases, behaviour, deterioration and treatment* (pp.
580 133–137). Valencia.

581 Mecklenburg, M. F., & Fuster Lopez, L. (2008). Failure mechanisms in canvas supported paintings:
582 approaches for developing consolidation protocols. In *Colore e conservazione: materiali e*
583 *metodi nel restauro delle opere policrome mobili: terzo congresso internazionale* (pp. 51–
584 60). Il prato.

585 Mecklenburg, M. F., McCormick-Goodhart, M., & Tumosa, C. S. (1994). Investigation into the
586 Deterioration of Paintings and Photographs Using Computerized Modeling of Stress
587 Development. *Journal of the American Institute for Conservation*, 33(2), 153–170.
588 <https://doi.org/10.2307/3179424>

589 Michalski, S. (1991). Paintings - Their Response to Temperature, Relative Humidity, Shock, and
590 Vibration. In M. Marion (Ed.), *Art in transit: Studies in the transport of paintings* (pp. 223–
591 248). National Gallery of Art.

592 Moon, R. J., Martini, A., Nairn, J., Simonsen, J., & Youngblood, J. (2011). Cellulose nanomaterials
593 review: structure, properties and nanocomposites. *Chemical Society Reviews*, 40(7), 3941–
594 3994. <https://doi.org/10.1039/C0CS00108B>

595 Nechyporchuk, O., Belgacem, M. N., & Bras, J. (2016). Production of cellulose nanofibrils: A
596 review of recent advances. *Industrial Crops and Products*, 93, 2–25.
597 <https://doi.org/10.1016/j.indcrop.2016.02.016>

598 Nechyporchuk, O., Belgacem, M. N., & Pignon, F. (2016). Current progress in rheology of
599 cellulose nanofibril suspensions. *Biomacromolecules*, 17(7), 2311–2320.
600 <https://doi.org/10.1021/acs.biomac.6b00668>

601 Nechyporchuk, O., Kolman, K., Oriola, M., Persson, M., Holmberg, K., & Bordes, R. (2017).
602 Accelerated ageing of cotton canvas as a model for further consolidation practices. *Journal*
603 *of Cultural Heritage*, 28, 183–187. <https://doi.org/10.1016/j.culher.2017.05.010>

604 Nechyporchuk, O., Pignon, F., & Belgacem, M. N. (2015). Morphological properties of
605 nanofibrillated cellulose produced using wet grinding as an ultimate fibrillation process.
606 *Journal of Materials Science*, 50(2), 531–541. <https://doi.org/10.1007/s10853-014-8609-1>

607 Nechyporchuk, O., Yu, J., Nierstrasz, V. A., & Bordes, R. (2017). Cellulose Nanofibril-Based
608 Coatings of Woven Cotton Fabrics for Improved Inkjet Printing with a Potential in E-Textile
609 Manufacturing. *ACS Sustainable Chemistry & Engineering*, 5(6), 4793–4801.
610 <https://doi.org/10.1021/acssuschemeng.7b00200>

611 Oriola, M., Možir, A., Garside, P., Campo, G., Nualart-Torroja, A., Civil, I., ... Strlič, M. (2014).
612 Looking beneath Dalí's paint: non-destructive canvas analysis. *Analytical Methods*, 6(1),
613 86–96. <https://doi.org/10.1039/C3AY41094C>

614 Ploeger, R., René de la Rie, E., McGlinchey, C. W., Palmer, M., Maines, C. A., & Chiantore, O.
615 (2014). The long-term stability of a popular heat-seal adhesive for the conservation of
616 painted cultural objects. *Polymer Degradation and Stability*, 107, 307–313.
617 <https://doi.org/10.1016/j.polymdegradstab.2014.01.031>

618 Rånby, B. G. (1949). Aqueous Colloidal Solutions of Cellulose Micelles. *Acta Chemica*
619 *Scandinavica*, 3, 649–650. <https://doi.org/10.3891/acta.chem.scand.03-0649>

620 Roche, A. (1993). Influence du type de chassis sur le vieillissement mecanique d'une peinture sur
621 toile. *Studies in Conservation*, 38(1), 17–24. <https://doi.org/10.1179/sic.1993.38.1.17>

622 Ryder, N. (1986). Acidity in canvas painting supports: Deacidification of two 20th century
623 paintings. *The Conservator*, 10(1), 31–36. <https://doi.org/10.1080/01410096.1986.9995015>

624 Santos, S. M., Carbajo, J. M., Gómez, N., Quintana, E., Ladero, M., Sánchez, A., ... Villar, J. C.
625 (2015). Use of bacterial cellulose in degraded paper restoration. Part I: application on model
626 papers. *Journal of Materials Science*, 1–12. <https://doi.org/10.1007/s10853-015-9476-0>

- 627 Shimizu, M., Saito, T., Fukuzumi, H., & Isogai, A. (2014). Hydrophobic, Ductile, and Transparent
628 Nanocellulose Films with Quaternary Alkylammonium Carboxylates on Nanofibril
629 Surfaces. *Biomacromolecules*, 15(11), 4320–4325. <https://doi.org/10.1021/bm501329v>
- 630 Stachurski, Z. H. (1997). Deformation mechanisms and yield strength in amorphous polymers.
631 *Progress in Polymer Science*, 22(3), 407–474. <https://doi.org/10.1016/S0079->
632 [6700\(96\)00024-X](https://doi.org/10.1016/S0079-6700(96)00024-X)
- 633 Stoner, J. H., & Rushfield, R. (2012). *Conservation of Easel Paintings*. Routledge.
- 634 Turbak, A. F., Snyder, F. W., & Sandberg, K. R. (1983). Microfibrillated cellulose, a new cellulose
635 product: Properties, uses, and commercial potential. *Journal of Applied Polymer Science:*
636 *Applied Polymer Symposium*, 37, 815–827.
- 637 Villers, C. (2004). Post minimal intervention. *The Conservator*, 28(1), 3–10.
638 <https://doi.org/10.1080/01410096.2004.9995197>
- 639 Völkel, L., Ahn, K., Hähner, U., Gindl-Altmutter, W., & Potthast, A. (2017). Nano meets the sheet:
640 adhesive-free application of nanocellulosic suspensions in paper conservation. *Heritage*
641 *Science*, 5, 23. <https://doi.org/10.1186/s40494-017-0134-5>
- 642 Wågberg, L., Decher, G., Norgren, M., Lindström, T., Ankerfors, M., & Axnäs, K. (2008). The
643 Build-Up of Polyelectrolyte Multilayers of Microfibrillated Cellulose and Cationic
644 Polyelectrolytes. *Langmuir*, 24(3), 784–795. <https://doi.org/10.1021/la702481v>
- 645 Wu, S.-Q., Li, M.-Y., Fang, B.-S., & Tong, H. (2012). Reinforcement of vulnerable historic silk
646 fabrics with bacterial cellulose film and its light aging behavior. *Carbohydrate Polymers*,
647 88(2), 496–501. <https://doi.org/10.1016/j.carbpol.2011.12.033>
- 648 Young, C. (1999). Towards a better understanding of the physical properties of lining materials for
649 paintings: Interim results. *The Conservator*, 23(1), 83–91.
650 <https://doi.org/10.1080/01410096.1999.9995142>

651 Young, C., & Jardine, S. (2012). Fabrics for the twenty-first century: As artist canvas and for the
652 structural reinforcement of easel paintings on canvas. *Studies in Conservation*, 57(4), 237–
653 253. <https://doi.org/10.1179/2047058412Y.0000000007>
654